CHEMISTRY & BIODIVERSITY

Accepted Article

Title: N-Sulfonyl-1,2,3,4-tetrahydroisoquinoline Derivatives: Synthesis, Antimicrobial Evaluations, and Theoretical Insights

Authors: Martín Rinaldi Tosi, Valeria Palermo, Fernando Giannini, Martín Fernández-Baldo, Jorge Diaz, Beatriz Lima, Gabriela Feresin, Guastavo Romanelli, and Héctor Armando Baldoni

To be cited as: *Chem. Biodiversity* **2023**, e202300905

Link to VoR: https://doi.org/10.1002/cbdv.202300905

N-Sulfonyl-1,2,3,4-tetrahydroisoquinoline Derivatives: Synthesis, Antimicrobial Evaluations, and Theoretical Insights

Martín E. Rinaldi Tosi,[+[a]] Valeria Palermo,[+[b]] Fernando A. Giannini,[[c]] Martín A. Fernández Baldo,[[d]] Jorge R. A. Díaz,[[c]] Beatriz Lima,[[e]] Gabriela E. Feresin,[[e]] Gustavo P. Romanelli,[[b,f]] and Héctor A. Baldoni*[[c,g]]

[a] Dr. Martín E. Rinaldi Tosi[+]
Laboratorio de Biotecnología y Tecnologías Biomédicas, Centro de Estudios para la Innovación y el Desarrollo (CEPID), Facultad de Ciencias Médicas, Universidad Católica de Cuyo, Felipe Velázquez 471 CP: 5700 Ciudad de San Luis, Argentina.
[b] Dra. Valeria Palermo[+], Dr. Gustavo P. Romanelli
Grupo de Investigación en Síntesis Orgánica Ecoeficiente (GISOE), Centro de Investigación y Desarrollo en Ciencias Aplicadas 'Dr. Jorge J. Ronco' (CINDECA), Departamento de Química, Facultad de Ciencias Exactas, Universidad Nacional de La Plata – CIC – CONICET, Calle 47 Nro 257, B1900AJK La Plata, Argentina.
[c] Dr. Fernando A. Giannini, Dr. Jorge R. A. Díaz
Área de Química General e Inorgánica, Departamento de Química, Facultad de Química, Bioquímica y Farmacia, Universidad Nacional de San Luis, Chacabuco 917, D5700BWS San Luis, Argentina.
[d] Dr. Martín A. Fernández Baldo
Universidad Nacional de San Luis, Facultad de Química, Bioquímica y Farmacia, Área de Química Analítica - Instituto de Química de San Luis, INQUISAL (UNSL – CONICET), Chacabuco 917, D5700BWS San Luis, Argentina.
[e] Dra. Beatriz Lima; Dra. Gabriela E. Feresin
Instituto de Biotecnología, Instituto de Ciencias Básicas, Universidad Nacional de San Juan, Av. Libertador General San Martin 1109 O, San Juan, Argentina.
[f] Dr. Gustavo P. Romanelli
CISAV. Cátedra de Química Orgánica, Facultad de Ciencias Agrarias y Forestales, Universidad Nacional de La Plata, Calles 60 y 119 s/n, B1904AAN La Plata, Argentina.
[g] Dr. Héctor A. Baldoni*
Instituto de Matemática Aplicada de San Luis, IMASL (UNSL – CONICET), Av. Italia 17556, D5700BYO San Luis, Argentina, http://www.unsl.edua.ar, *E-mail:* *hbaldoni@unsl.edu.ar*

Abstract

Microbial contamination remains a significant economic challenge in the food industry, emphasizing the need for innovative antimicrobial solutions. In this study, we synthesized *N*-sulphonyl-1,2,3,4-tetrahydroisoquinolines (NSTHIQ) derivatives using an environmentally friendly Preyssler heteropolyacid catalyst, obtaining moderate to high yields (35-91%) under mild conditions. Two derivatives (**5** and **6**) exhibited significant antifungal properties against various fungal species, including *Aspergillus spp*, *Penicillium spp*, and *Botrytis cinerea*. ADMET (Absorption, Distribution, Metabolism, Excretion, and Toxicity) analysis revealed the absence of hepatic toxicity in all compounds, making derivatives **2**, **3**, **4**, and **5** potential candidates for further development. However, derivatives **6** and **7** exhibited immunotoxicity. In support of our experimental findings, reactivity indices were computed using Density Functional Theory principles, deriving valuable insights into the chemical properties of these derivatives. This study underscores the potential of NSTHIQ compounds as potent antifungal agents, coupled with the importance of employing environmentally friendly catalysts in drug discovery.

Introduction

Food loss and waste resulting from chemical or biological contamination pose a significant global food challenge, impacting not only the source materials but also the derived products. While chemical contamination risks are more prominent in conventionally farmed products, organic farming carries a higher likelihood of biological contamination. Furthermore, food degradation caused by contamination from various microorganisms is the leading cause of economic losses within the food supply chain. This issue primarily affects the post-harvest phase and has repercussions throughout the entire food production chain, encompassing farmers, warehouse operators, sellers, and consumers

at different stages, including production and pre-harvest, harvesting and initial handling, storage, transportation, processing, retail, and consumption. According to the Food and Agriculture Organization (FAO), the matter of food security holds implications not only for public health but also for government oversight and regulatory agencies.[1]

Phytopathogenic fungi can colonize crops and generate mycotoxins within the edible parts of plants. These mycotoxins can accumulate in infected food products, posing a significant risk to both human and animal health. When these mycotoxins come into contact with or are ingested by individuals, they can have adverse effects on their health. As a result, these fungi and the toxins they produce are responsible for numerous cases of mycotoxicosis. Furthermore, these mycotoxins have been identified as carcinogens that promote the development of tumours, particularly hepatocarcinoma, and they also exhibit strong allergenic properties. [2]

Various fungi are known to cause postharvest diseases in food crops. Notably, *Aspergillus spp*. and *Penicillium spp*. are two prominent genera in this regard. While these fungi are commonly found in soil and air and are generally considered saprophytic, some species within these genera can cause deterioration during food storage, plant diseases, or even invasive diseases in animals and humans. *Alternaria spp*. are primarily saprophytic fungi, but certain species have developed pathogenic capabilities, collectively causing diseases across a wide range of hosts. *Botrytis cinerea* often referred to as "grey mold," produces various toxins and possesses virulence factors that lead to rapid plant tissue death and decomposition. Lastly, *Fusarium spp.* constitutes a genus of filamentous fungi with considerable agricultural importance. They are known for being plant pathogens, producers of mycotoxins, and opportunistic human pathogens. These genera were selected for their global significance from both biochemical and economic perspectives and represent some of the most common culprits associated with food spoilage and mycotoxin production.[3]

The control of these postharvest diseases primarily relies on agricultural pesticides. Nevertheless, the ongoing application of these substances has led to growing resistance in fungal populations, making eradication increasingly challenging. In light of this situation, there is a global drive to identify novel antimicrobial agents that exhibit enhanced efficacy, particularly against microbial strains that have developed resistance to all presently known antimicrobial agents.[4]

Therefore, it is imperative to develop novel antifungal agents and improve existing ones for the benefit of both agriculture and human health. Nevertheless, the concurrent increase in antimicrobial drug resistance, exacerbated by the indiscriminate use of antimycotic treatments, underscores the urgent necessity for a broader range of medications to effectively combat fungal infections.

N-sulphonyl-1,2,3,4-tetrahydroisoquinoline (NSTHIQ) derivatives represent a common structural element found in a diverse array of biologically active natural compounds and pharmaceutical substances. Furthermore, their utility in treating various diseases, such as Parkinson's, leukaemia, Alzheimer's, acquired immunodeficiency syndrome (AIDS), and melanoma, has been documented.[5]

On the other hand, sulfonamide groups are widely recognized for their diverse biological properties, which encompass anticancer, antiviral, antibacterial, antihypertensive, and antiepileptic effects.[6] The NSTHIQ derivatives, which combine isoquinolines and sulfonamides, have demonstrated their utility in various medical applications, and numerous biologically active compounds featuring this substructure exhibit a wide range of pharmacological effects.[5,6]

The traditional synthesis of NSTHIQ derivatives involves the Pictet-Spengler reaction. This process includes the condensation of *N*-sulphonyl-phenylethylamine with a carbonyl compound, followed by an intramolecular aromatic electrophilic substitution.[7]

This reaction typically occurs in a strong acid environment or supported Wells-Dawson, Preyssler, and Keggin heteropolyacids.[8,9]

Preyssler heteropolyacids are characterized by the general formula $H_xA_y[B_5D_{30}O_{110}]\cdot zH_2O$, where x, y, and z fall within the following ranges: $0<x<15$, $0<y<15$, and $0<z<50$. These compounds feature a cyclic structure that originates from the Keggin anion ($BD_{12}O_{40}^{3-}$) through the removal of two sets of three corner-sharing DO_6 octahedra. Some examples within this family include $H_{14}NaP_5W_{30}O_{110}$ and $H_{14}NaP_5W_{29}MoO_{110}$ (PWMo).[10,11] Preyssler heteropolyacids serve as efficient and environmentally friendly catalysts due to their strong Brönsted acidity, hydrolytic stability, low corrosiveness, ease of recovery, and minimal waste production. They have a wide range of applications, including catalyzing the selective oxidation of alcohols and aldehydes, ammoxidation of 2-methylpyrazine, aerobic oxidation of H_2S, esterification of alcohols, etherification of hydroxymethylfurfural, and facilitating the synthesis of diverse heterocycles through multicomponent reactions, such as phenylcoumarins and pyrroles, among others reactions.[10,12]

In this study, was utilized a Preyssler bulk solid, specifically PWMo, as an environmentally friendly and recyclable catalyst for synthesizing NSTHIQ derivatives. These newly synthesized compounds were assayed for their potential antifungal properties against a range of *Aspergillus* species (*A. niger*, *A. flavus*, *A. parasiticus*, and *A. ochraceus*), *Penicillium* species (*P. expansum* and *P. verrucosum*), *Alternaria* species (*A. alternate* and *A. tenuissima*), *Botrytis cinerea*, and *Fusarium oxysporum*. Additionally, we evaluated the compounds for their antibacterial activity against both Gram-positive *Staphylococcus aureus* strains and Gram-negative *Escherichia coli* strains. Furthermore, we conducted drug-likeness assessments based on Lipinski's "Rule of Five," examined ADME (Absorption, Distribution, Metabolism, and Elimination) properties, assessed

toxicological risks, and calculated reactivity indices using theoretical Density Functional Theory (DFT).

Results and Discussion

Chemistry

All derivatives included in this study are known and they were resynthesized, purified, and characterized to evaluate the biological activity.[12] The synthetic route to obtain the NSTHIQ derivatives **2** to **7** is shown in *Scheme 1*. The synthesis was accomplished in high yield by a Preyssler bulk solid PWMo as a green recyclable catalyst.

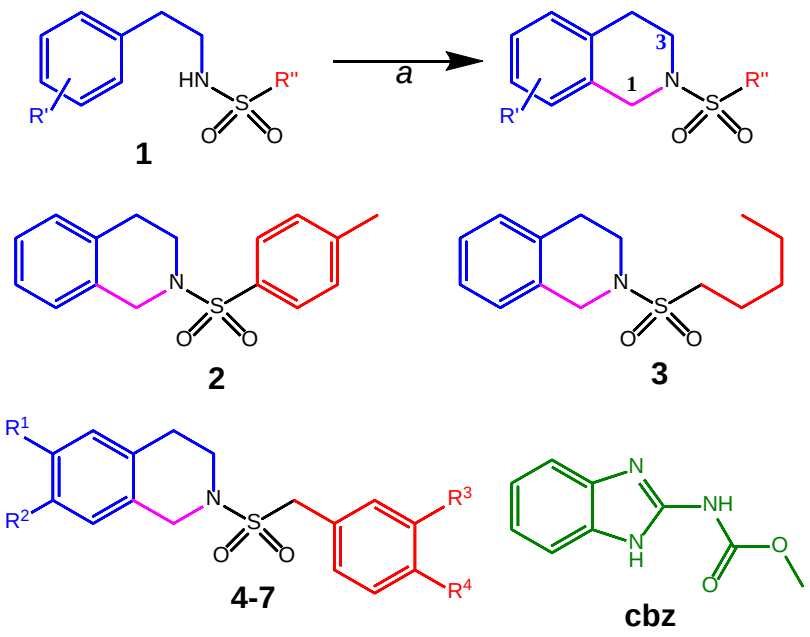

4: R^1=R^2=R^3=H; R^4=Cl **6**: R^1=H,R^2=OMe; R^3=R^4=Cl

5: R^1=R^2=H; R^3=R^4=Cl **7**: R^1=R^2=OMe; R^3=R^4=Cl

Scheme 1. Synthesis of the NSTHIQ derivatives **2** to **7**. [a] Unless otherwise mentioned, reaction was carried out with sulfonamide (1 mmol), trioxane (3 mmol), toluene (2 mL), catalyst PWMo 1%mmol, at 70ºC, 30 min., and stirring.

All synthetized compounds were insoluble in water but soluble in organic solvents like *N*,*N*-dimethylformamide (DMF) and dimethylsulfoxide (DMSO). The synthesized compounds were off-white solids with relatively high melting points. The structures of

them (*Scheme 1*) were determined and characterized by different experimental spectroscopic techniques such as ^{1}H-NMR, ^{13}C-NMR, and MS. For spectral data, and spectra, please see the *Supporting Information*. In addition, theoretical computation of ^{1}H- and ^{13}C-NMR signal assignations are companying the experimental data.[13] This comparison is not only to make the entire signals assignation straightforward but also to guarantee unbiased experimental information. It is noteworthy that a remarkable concordance exists when comparing the experimental ^{1}H- and ^{13}C-NMR chemical shift spectra with the calculated ones. The coefficient of determination (denoted as R^2) is approximately 0.99 for both ^{1}H-NMR and ^{13}C-NMR chemical shifts in their respective datasets, as shown in *Figure S1*. Indeed, it is important to highlight that experimental results stem from overlapping spectra of low-energy conformers of the compounds in solution. Conversely, for the theoretical spectrum calculations, we adopted a gauche conformation for the sulfonamide C^{1}-N-S-R" rotation, as previously determined.[14, 15]

Antifungal activity evaluation

Table 1 shows that derivative **2**, **5**, and **6** exhibit significant antifungal activities. Our results indicate that compound **2** exhibits a substantial antifungal effect, specifically of 73.3% against *B. cinerea*. Compound **5** demonstrates significant antifungal activity of 77.8% and 94.1% against *A. flavus* and *A. parasiticus*, respectively. It also inhibits the growth of other pathogens, namely *P. expansum* (73.2%) and *P. verrucosum* (80.9%). Additionally, compound **5** exhibits antifungal activity of 66.7% against *B. cinerea*. Compound **6** demonstrates noteworthy overall antifungal efficacy, with inhibitions of 71.4%, 63.9%, 73.5%, and 82.1% against *A. niger*, *A. flavus*, *A. parasiticus*, and *A. ochraceus*, respectively. However, it is important to note that none of the synthesized

derivatives exhibit significant antifungal activity against *A. alternata*, *A. tenuissima*, or *Fusarium oxysporum*.

Table 1. Percent antifungal activity.

	Compound					
Fungi	**2**	**3**	**4**	**5**	**6**	**7**
Aspergillus ssp.						
A. niger	35.71	46.43	32.14	39.29	71.43	53.57
A. flavus	16.67	27.78	25.00	77.78	63.89	22.22
A. parasiticus	20.59	29.41	26.47	94.12	73.53	26.47
A. ochraceus	32.14	32.14	32.14	50.00	82.14	28.57
Penicillium ssp.						
P. expansum	24.39	31.71	41.46	73.17	21.95	46.34
P. verrucosum	33.33	30.95	35.71	80.95	38.10	40.48
Alternaria ssp.						
A. alternata	33.33	29.63	22.22	37.04	14.81	33.33
A. tenuissima	34.62	34.62	30.77	38.46	26.92	34.62
Botrytis ssp.						
B. cinerea	73.33	53.33	46.67	66.67	53.33	60.00
Fusarium ssp.						
F. oxysporum	25.71	22.86	28.57	31.43	20.00	34.29

Antibacterial activity evaluation

The results of the antibacterial assays conducted on compounds **2** to **7** revealed that the MICs values were higher than 50 µg/mL (*Table 2*). These results indicate that the assayed compounds were inactive against the selected bacteria.

10.1002/cbdv.202300905

Table 2. Antibacterial activity.

	Compound MIC (μg/mL)							
Microorganisms	**2**	**3**	**4**	**5**	**6**	**7**	**CTX**	**IPM**
Gram (+)								
Staphylococcus aureus methicillin-sensitive ATCC 25923	>50	>50	>50	>50	>50	>50	0.5	0.5
Staphylococcus aureus methicillin-resistant ATCC 43300	>50	>50	>50	>50	>50	>50	0.5	0.5
Gram (-)								
Escherichia coli ATCC 25922	>50	>50	>50	>50	>50	>50	0.25	0.5
Escherichia coli 11089	>50	>50	>50	>50	>50	>50	0.25	0.5

Abbreviations: CTX, cefotaxime; IPM, imipenem.

Computational studies

Drug-likeness profile

The compounds underwent a comprehensive assessment for their drug likeness profile, as detailed in *Table S1*. In terms of solubility, as determined by LogS, compounds **2** to **7** are categorized as moderately to poorly soluble in water (-5.601<LogS<-4.145), whereas **cbz** is anticipated to be soluble in water (LogS≈-1.829). Furthermore, the partition coefficient LogP values range from 3.654 to 4.501 for compounds **2** to **7**, whereas **cbz** is predicted to have a LogP≈1.391. This high LogP suggests the hydrophobic nature of **2** to **7**, facilitating their solubility in lipids.[16] These findings, in conjunction with other physicochemical descriptors, indicate significant oral bioavailability. Notably, none of the derivatives violated drug-likeness rules and all adhered to the Rule of Five (RO5). For a rapid overview of their drug-likeness, a bioavailability radar plot is presented in *Figure 1*, showcasing six different physicochemical properties: lipophilicity, size, polarity, solubility, flexibility, and saturation.[17]

10.1002/cbdv.202300905

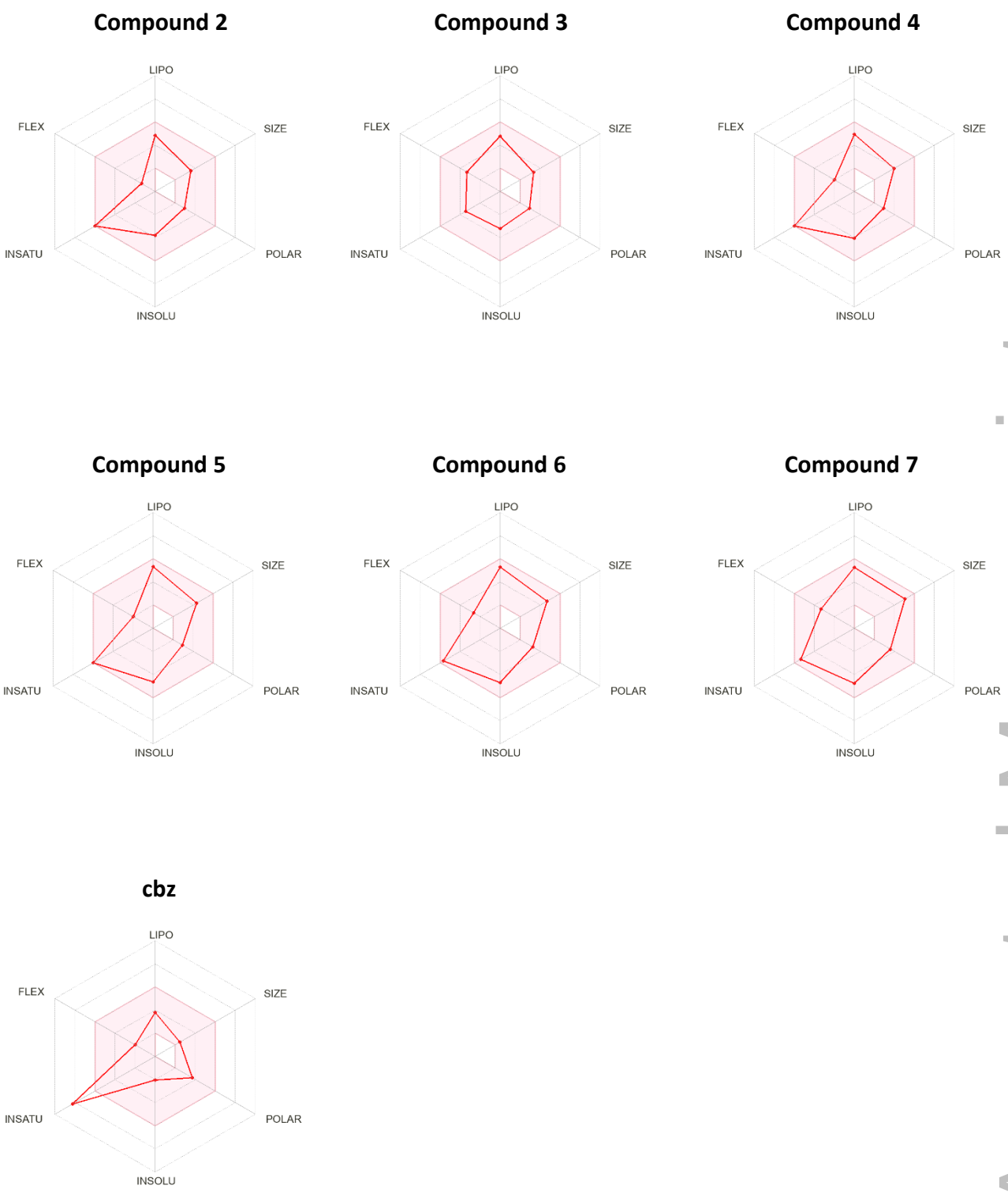

Figure 1. Bioavailability radar plot. Six physicochemical properties are taken into account (i.e. LIPOphilicity, SIZE, POLARity, INSOLUbility, INSATUration, and FLEXibility. Physicochemical range on each axis is depicted as a pink area in which the radar plot of the target compound has to fall entirely to be considered drug-like.

Pharmacokinetics analysis

The pharmacokinetic data, as listed in *Table S2*, indicate that all compounds exhibit high levels of passive gastrointestinal absorption (GIA) and passive permeation across the blood-brain barrier (BBB). Furthermore, these compounds are predicted to be unaffected by active efflux P-gp proteins (PGP−). These critical ADME parameters, namely GIA, BBB permeation, and P-gp binding, are depicted in a boiled-egg diagram in *Figure 2*.[17] Pharmacokinetic analysis suggests that compounds **2** to **7** could serve as substrates for CYP-mediated metabolic biotransformations.[18]

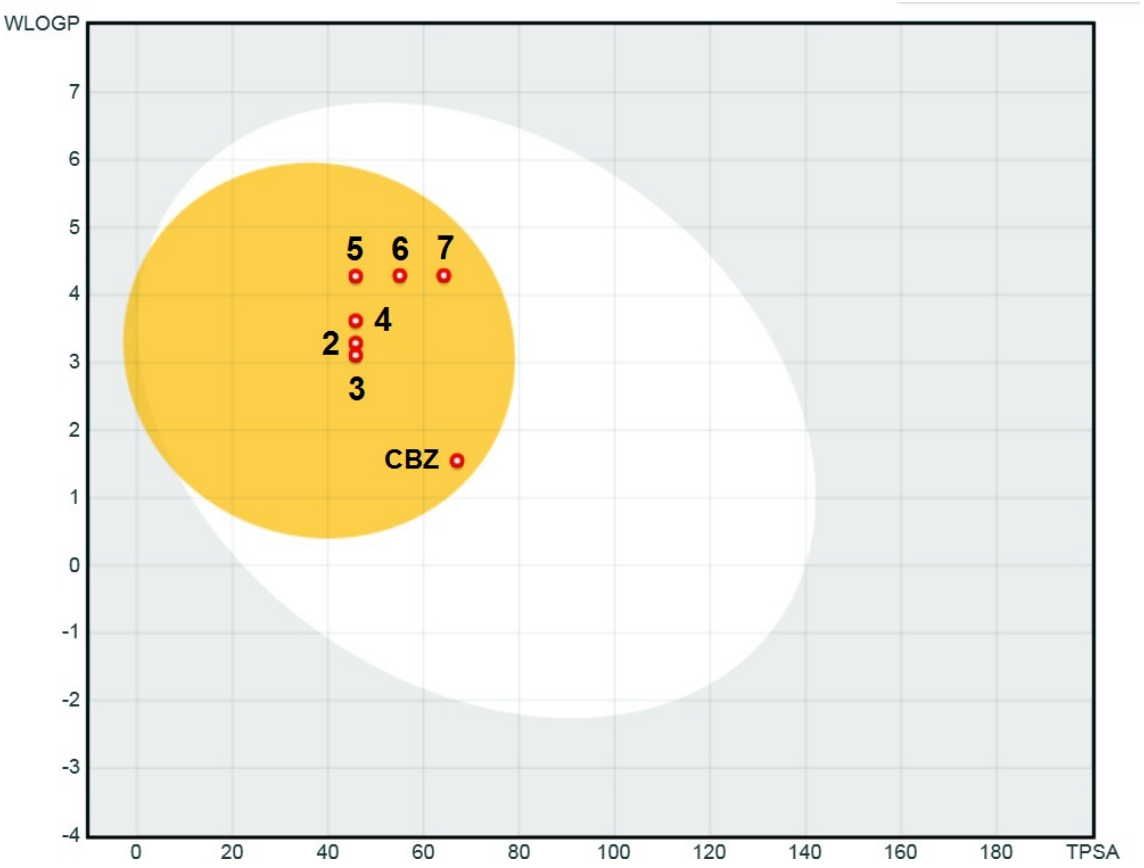

Figure 2. Boiled-egg diagram.

Toxicological Risks

We assessed the potential toxicity of compounds **2** to **7** using machine-learning models designed to predict various toxicity endpoints.[19] The corresponding data is presented in *Table S3*.

Compound **2** is estimated to have an LD_{50} of 2500 mg/kg and falls into acute oral toxicity class 5, as predicted. This compound is expected to exhibit inactivity across twelve toxicological pathways, four toxicological endpoints, and hepatotoxicity. However, Opioid receptor mu is identified as a potential toxicity target. Compounds **3**, **4**, and **5** are predicted to have LD_{50} values of 541 mg/kg, 780 mg/kg, and 800 mg/kg, respectively, categorizing them as acute oral toxicity class 4. These compounds are also anticipated to be inactive across the twelve toxicological pathways and hepatotoxicity. No binding to any of the 15 toxicity targets[19] is anticipated for compounds **3** to **7**. Compounds **6** and **7** are expected to fall into toxicity class 4, each with an LD_{50} value of 940 mg/kg. They are predicted to exhibit immunotoxicity with high confidence scores of 0.67 and 0.72, respectively, and no binding to any of the 15 toxicity targets is foreseen for these compounds. Lastly, reference compound **cbz** is predicted active for hepatotoxicity and mutagenicity. This compound is also predicted as active for nuclear receptor signaling and stress response pathways. These findings align perfectly with prior research, which has demonstrated that **cbz** can lead to embryotoxicity, apoptosis, teratogenicity, infertility, hepatocellular dysfunction, endocrine-disrupting effects, disruption of haematological functions, mitotic spindle abnormalities, mutagenicity, and aneugenicity effects. These effects have been documented in both acute and delayed experiments.[20]

In summary, our research indicates that none of the NSTHIQ derivatives display hepatotoxicity. Additionally, compounds **2**, **3**, **4**, and **5** emerge as potential safe derivatives based on our results. These compounds exhibited inactivity in various nuclear receptor signalling and stress response pathways. Conversely, derivatives **6** and **7** are predicted to exhibit immunotoxicity, and therefore, we do not categorize them as safe options.

Reactivity descriptors

The reactivity of a substrate stands as the foremost determinant in enzyme-mediated biotransformations. Consequently, one can formulate atomic and molecular reactivity indices through the utilization of electronic descriptors derived from quantum chemistry methodologies. To achieve this, optimized geometries at the IEFPCM-B3LYP-GD3BJ/6-311+G(2d,p) level of theory, were scrutinized with a focus on characterizing them as minima (i.e. no imaginary frequencies found) through frequency calculations. The optimized coordinates at the local conformational minimum are provided in *Table S4*, and selected energy values related to the local minimum conformation have been compiled in *Table S5*.

Given that valence electrons move through reactive orbitals during chemical reactions, Fukui's frontier orbital theory highlights the significance of the highest occupied molecular orbital (HOMO) and the lowest unoccupied molecular orbital (LUMO) in comprehending chemical reactivity.[21] The global chemical reactivity properties, derived from a topological analysis of Fukui functions (TAFF), have been documented in *Table 3* for reference.[22]

Table 3. Global chemical reactivity.

	Compound						
Index[a]	**2**	**3**	**4**	**5**	**6**	**7**	**cbz**
HOMO energy	-0.253	-0.253	-0.253	-0.254	-0.229	-0.239	-0.228
LUMO energy	-0.049	-0.026	-0.042	-0.049	-0.049	-0.049	-0.034
GAP	0.204	0.228	0.211	0.205	0.180	0.190	0.194
Ionization potential	0.253	0.253	0.253	0.254	0.229	0.239	0.228
Electroaffinity	0.049	0.026	0.042	0.049	0.049	0.049	0.034
Chemical potential	-0.151	-0.140	-0.148	-0.152	-0.139	-0.144	-0.131
Global Hardness	0.102	0.114	0.106	0.102	0.090	0.095	0.097
Global Softness	4.894	4.395	4.739	4.879	5.559	5.272	5.145
Electronegativity	0.151	0.140	0.148	0.152	0.139	0.144	0.131
Electrophilicity Index	0.112	0.086	0.103	0.112	0.108	0.110	0.088
w- Electron Donator	0.200	0.170	0.190	0.201	0.188	0.193	0.166
w+ Electron Acceptor	0.049	0.030	0.043	0.049	0.049	0.049	0.035
Electrophilicity Net	0.249	0.200	0.233	0.250	0.238	0.243	0.200

[a] in atomic units (a.u.)

The energy gap between the HOMO and LUMO provides insights into diverse charge-transfer possibilities within the molecules under consideration. Specifically, for molecules **2** to **7**, the determined energy gap values were as follows: 0.204, 0.228, 0.211, 0.205, 0.180, and 0.190 atomic units, respectively (*Table 3*). Based on these outcomes, it is evident that compounds **3** and **6** exhibit the highest and lowest stability, respectively. In particular, the analysis using TAFF suggests that compound **6** possesses the smallest HOMO-LUMO gap, presumably indicating a correlation with the observed biological activity. On another hand, global softness, denoted as the reciprocal of global hardness, serves as a metric for assessing polarizability, and the information gleaned from the total molecular softness is particularly well-suited for the analysis of inter- and intramolecular reactivity.[23] Notably, in *Table 3*, we observe that Compound **6** exhibits the highest global softness among the compounds examined. Furthermore, as depicted in *Table 3*, the active compounds, **5** and **6**, have higher net electrophilicity. Net electrophilicity measures a species' ability to acquire electrons about its capacity to

donate them.[24] It is worth highlighting that numerous chemical toxicants and their active metabolites are electrophilic, thereby causing cellular harm by forming covalent bonds with nucleophilic targets on biological macromolecules.[25] In summary, our results suggest that Compounds **2**, **5**, **6**, and **7** possess global softness and net electrophilicity levels comparable to, or higher than, the reference compound **cbz**.

Although global indices can offer valuable insights into reactivity across an entire system, we have directed our attention towards local properties aiming to comprehend the factors influencing chemical selectivity.[26] In *Figure 3*, we present sketches illustrating the Fukui function topology for nucleophilic (f+) and electrophilic (f-) attacks on active compounds **5** and **6**. As expected, the benzylsulphonyl framework acts as an electron-withdrawing group, resulting in more pronounced overall electron withdrawal effects, particularly in the presence of halogen substitution.[27] In contrast, the tetrahydroisoquinoline scaffold acts as a weaker electron-donating base. This is attributed to the nitrogen atom in tetrahydroisoquinoline, whose electron pair is firmly held due to its delocalization within the π system of the aromatic ring. Furthermore, in our findings, the maxima of the Fukui functions could be linked to the primary sites of metabolic attacks and highly reactive electrophilic oxidants in cytochromes, as extensively discussed elsewhere.[28,29]

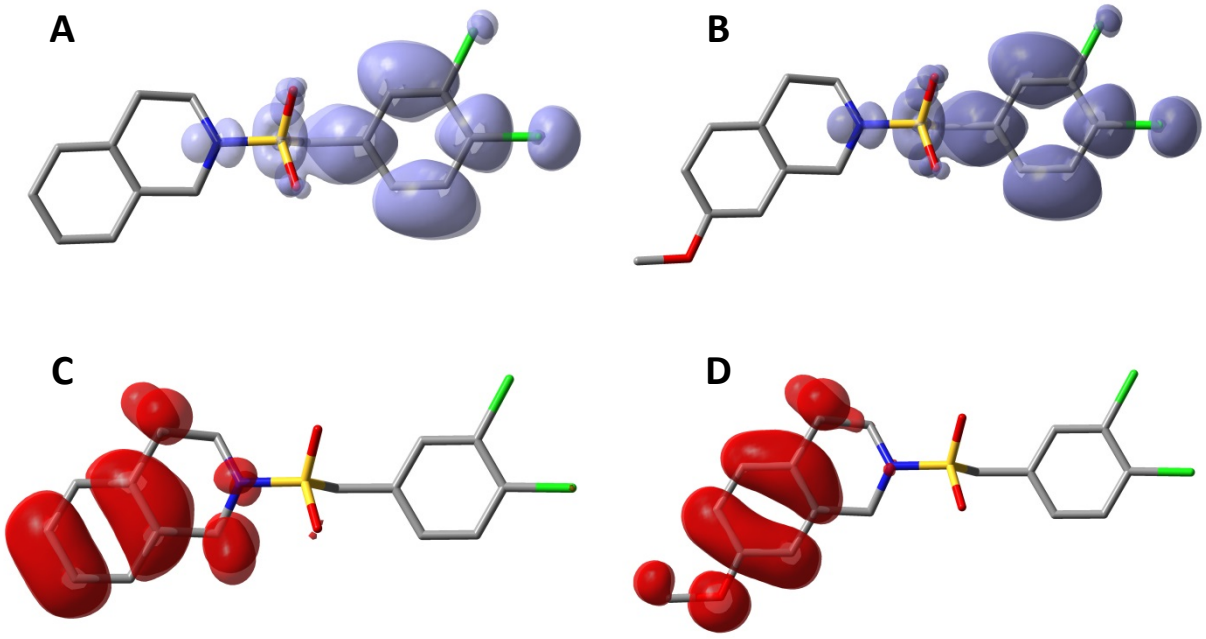

Figure 3. Electron acceptor isosurfaces (f+) in blue, and electron donor isosurfaces (f–) in red. This applies to both compound **5** (sketches A and C) and compound **6** (sketches B and D). The isosurfaces are depicted with a contour level set at 0.006 atomic units.

Conclusions

In the present study, we have successfully synthesized six derivatives of NSTHIQ employing an environmentally friendly Preyssler heteropolyacid catalyst. These derivatives were obtained with moderate to good yields, swift reaction times, and mild reaction conditions, all achieved with the assistance of a non-corrosive solid catalyst. Upon in vitro assessment of derivatives **5** and **6**, we uncovered significant antifungal activity against various fungal species, including *Aspergillus spp*, *Penicillium spp*, and *Botrytis cinerea*. However, it is worth noting that none of the derivatives exhibited antibacterial activity. Additionally, an ADMET (Absorption, Distribution, Metabolism, Excretion, and Toxicity) analysis indicated the absence of hepatic toxicity

in all synthetized derivatives. Moreover, compounds **2**, **3**, **4**, and **5** may be considered as potentially safe derivatives. In contrast, derivatives **6** and **7** are predicted to possess immunotoxicity. To complement these experimental findings, reactivity indices computations were carried out using conceptual Density Functional Theory, which, to a certain extent, substantiated our findings.

Experimental Section

Experimental

Chemicals were purchased from chemical companies such as Aldrich and Fluka and were freshly used after purification by standard procedures (distillation and recrystallization), TLC monitored all the reactions. The yields were calculated from purified compounds. The synthetized products were identified by comparing physical data previously reported.[30-32] Melting points were determined in sealed capillary tubes and were uncorrected. Room temperature ^{1}H- (400.1 MHz) and ^{13}C- (100.6 MHz) NMR measurements were performed on a Bruker Avance DPX-400 spectrometer. The chemical shift standard was internal tetramethylsilane for ^{1}H- and ^{13}C-NMR. The following abbreviations were used for chemical shift multiplicities spectra: br s=broad singlet, br d=broad doublet, br m=broad multiplet, s=singlet, d=doublet, t=triplet, q=quartet, sep=septet, m=multiplet, ps=pseudo. Experimental ^{1}H-NMR and ^{13}C-NMR signals assignations are accompanied by neural networks predicted chemical shifts spectral data[13] to guarantee and corroborate unbiased signals assignments. MS was measured by VG Autospec mass spectrometer.

Synthesis of Preyssler catalyst

The catalyst was prepared using established methods.[10,33] To synthesize the potassium salt, we dissolved $Na_2WO_4 \cdot 2H_2O$ (23.0 g, 0.07 mol) and $Na_2MoO_4 \cdot 2H_2O$ (2.0 g, 0.008 mol) in 20 mL of hot distilled water, employing reflux with continuous stirring. Subsequently, H_3PO_4 (85%, 27 mL, 0.02 mol) was slowly added and the mixture was refluxed for 24 hours. Following this, we introduced HNO_3 (70%, 1 mL) and KCl (10 g, 0.13 mol) into the mixture, and it was stirred. The resulting suspension underwent centrifugation for 15 minutes. The solid obtained was dissolved in 50 mL of hot distilled water and allowed to cool overnight at approximately 4 ºC. The resulting $K_{14}[NaP_5W_{29}MoO_{110}]$ was filtered and vacuum-dried at room temperature to yield Preyssler acid (PWMo). The potassium salt solution was passed through a Dowex® 50Wx8 ion-exchange column, and the exchanged solution was subsequently dried in an air column. The solid underwent comprehensive characterization using various techniques, including Fourier transform infrared spectroscopy, diffuse reflectance spectroscopy, X-ray diffraction, scanning electron microscopy, textural analysis (S_{BET}) via nitrogen adsorption/desorption, and potentiometric titration. The characterization results confirmed the effective synthesis of Preyssler PWMo, consistent with prior reports.[33]

Catalytic synthesis of NSTHIQ

In our experimental setup, we utilized a round-bottom flask equipped with a condenser. The reactants, specifically *N*-phenyl-ethylsulfonamide (**1**), trioxane, and PWMo, were employed in quantities of 1 mmol, 3 mmol, and 1% mmol, respectively. The *N*-phenyl-ethylsulfonamide (**1**) was obtained from a previous study.[30]

To initiate the reaction, the mixture was dissolved in 2 mL of toluene and stirred at 70 ºC for of 30 minutes. Subsequently, an additional 10 mL of solvent was introduced, and the catalyst was separated via filtration, followed by a thorough wash with toluene. The resulting solution underwent desiccation using anhydrous Na_2SO_4 and was then filtered. The solvent was evaporated, yielding the product (compounds **2** to **7**), which was subsequently purified through recrystallization using either acetone or ethyl acetate to attain pure compounds. The structural elucidation of the obtained compounds was carried out using spectroscopic techniques, including ^{1}H- and ^{13}C-NMR, as well as mass spectrometry (MS).

Monosporic cultures of microorganisms

In our investigation of antifungal activity, we examined the impact on several fungal species, including four distinct *Aspergillus* species (*A. niger*, *A. flavus*, *A. parasiticus*, and *A. ochraceus*), two *Penicillium* species (*P. expansum* and *P. verrucosum*), two *Alternaria* species (*A. alternate* and *A. tenuissima*), as well as *Botrytis cinerea* and *Fusarium oxysporum*. These fungi were cultivated in tilted tubes on potato dextrose agar (PDA) from Sigma-Aldrich, USA, and were allowed to grow for a period of 5 days at a temperature of 22 °C. Subsequently, they were isolated and purified through monosporic culture in the following manner: Conidia were reconstituted in microtubes containing 1 mL of 0.1% Tween 80 under aseptic conditions, creating a suspension for each tube containing the growing fungi. This suspension was then subjected to vortexing three times for 15 seconds each, and the spore count was determined using a Neubauer chamber. Finally, dilutions of each suspension were prepared, resulting in a final concentration of $1x10^5$ spores/mL for each monosporic culture.

Assessment of antifungal activity by Growth inhibitory assay

Agar-well diffusion susceptibility test

We assessed the antifungal activity of the NSTHIQ compounds using the agar well diffusion method. In this procedure, 100 µL suspensions of each studied fungal strain were evenly spread onto Petri dishes with a diameter of 15 cm, pre-filled with potato dextrose agar (PDA), and distributed using a Drigalski spatula within a laminar flow cabinet. For each chemical compound under examination, three plates were employed. In each of these plates, three wells, each measuring 6 mm in diameter, were aseptically created. Subsequently, these wells were filled with 50 µL of a test compound solution, with different dilutions prepared in triplicate. These compounds were initially dissolved in DMF to achieve final concentrations of 1, 5, and 10 mM/mL. To ensure sterility, the solutions were subsequently filtered using a 0.22 µm filter. All Petri dishes were then incubated at a temperature of 22 °C for 4 days. After this incubation period, we measured the radial growth of the mycelium for each respective microorganism and determined the corresponding inhibition zones' diameters in millimetres (*Table S6*). Concurrently, control experiments were conducted, including negative controls using DMF without any antibiotic and positive controls utilizing carbendazim (**cbz**) dissolved in DMF, a systemic polyvalent fungicide. We repeated each experiment a minimum of three times to ensure consistency. The results were expressed as the percentage of mycelium growth inhibition relative to the carbendazim control, where 100% inhibition represented the level achieved by carbendazim. Compounds were classified as active if the percentage of mycelium growth inhibition, in comparison to carbendazim, exceeded 60%.

Antibacterial activity

Reference strains from the American Type Culture Collection (ATCC) were chosen for this study, encompassing two Gram-positive bacterial strains, methicillin-sensitive Staphylococcus aureus ATCC 25923 (MSSA) and methicillin-resistant Staphylococcus aureus ATCC 43300 (MRSA), as well as the Gram-negative Escherichia coli (EC) strains ATCC 25922 and ATCC 11089. Each strain underwent overnight cultivation in Mueller-Hinton broth. The inoculum concentration employed ranged from 1 to 5×10^5 colony forming units per millilitre (CFU/mL), adhering to the guidelines set forth by the Clinical and Laboratory Standards Institute.[34] For the determination of Minimal Inhibitory Concentration (MIC) of compounds **2** to **7**, the broth microdilution technique was employed. Stock solutions of each compound in dimethylsulphoxide (DMSO) were prepared and subsequently diluted to create serial twofold dilutions.[34] These dilutions were then added to the respective culture media to achieve final concentrations spanning from 1 to 100 μg/mL. The final concentration of DMSO in the assay did not exceed 1%. As positive controls, the assays included the antimicrobial agents Cefotaxime® (Argentia Pharmaceutica) and Imipinem (Laboratorio NORTHIA Argentina). The microplates, each containing 96 wells, underwent 24-hour incubation at 37 °C, with the effects evaluated using a spectrophotometer, measuring absorbance at 620 nm with the Multiskan FC instrument. Tests were made in triplicate and MIC values are expressed as μg/mL.

Computational analysis

Drug-likeness profile

The Rule of Five (RO5), which evaluates a chemical compound's drug-likeness, is based on specific physicochemical parameters. These parameters include a molecular

weight (MW) less than 500 Dalton, high lipophilicity assessed by a ClogP value ≤ 5, fewer than 5 hydrogen bond donors (HBD), fewer than 10 hydrogen bond acceptors (HBA), and a molar refractivity (MR) within the range of 40-130.[35] This guideline serves as a general framework to determine whether a chemical compound possesses the requisite chemical and physical attributes for potential oral drug activity in humans. [35, 36] To assess the drug-likeness profile, we employed the SwissADME web tool in conjunction with the ADMETlab website.[17,37]

ADME analysis

The primary causes of drug development failures often stem from unfavourable pharmacokinetics profiles in drug-likeness candidates. Consequently, it is imperative to undertake early evaluations of a compound's potential suitability as a drug to enhance research and development efficiency. Presently, assessing ADME (Absorption, Distribution, Metabolism, and Excretion) characteristics typically entails resource-intensive, time-consuming processes and often necessitates extensive animal experimentation. Consequently, computer-based modelling techniques have emerged as the preferred approach in the initial phases of drug discovery for ADME prediction. To assess the ADME profile, we utilized the SwissADME web tool and the pkCSM server.[17,38]

Toxicological Risks

To predict the toxicological risks associated with selected compounds using structural models, we employed the ProTox-II web server.[19,39] This tool encompasses molecular similarity, pharmacophores, fragment propensities, and machine-learning models for predicting various toxicity endpoints. [19,39] For the NSTHIQ derivatives, we

computed the following toxicity endpoints: 1) Acute toxicity, including toxicity classes, oral LD50, and predicted accuracy percentage. 2) Organ toxicity, specifically hepatotoxicity. 3) Various toxicological endpoints, encompassing carcinogenicity, immunotoxicity, mutagenicity, and cytotoxicity. 4) Toxicological pathways, divided into nuclear receptor signalling pathways (such as aryl hydrocarbon receptor, androgen receptor, and peroxisome proliferator-activated receptor gamma) and stress-response pathways (including nuclear factor erythroid-derived 2-like 2/antioxidant responsive element, heat shock factor response element, mitochondrial membrane potential, phosphoprotein p53, and ATPase family AAA domain-containing protein 5); and finally 5) Toxicity targets, which comprised 15 distinct models.[19,39,40] Compounds predicted to carry a toxicological risk were categorized as "Active," along with their associated confidence scores for such events. Conversely, compounds devoid of any predicted toxicological risk were classified as "Inactive." Notably, compounds falling into the "Inactive" category are more likely to exhibit effectiveness in subsequent *in vitro* and *in vivo* experiments.

Density Functional Theory (DFT) calculations

DFT calculations were conducted for all compounds, involving modelling and energy minimization. These calculations were executed using the Gaussian 16 program.[41] We employed the B3LYP DFT functional coupled with homogenous 6-311+G(2d,p) Pople-style orbital basis sets.[42,43] To accurately account for noncovalent and dispersion interactions, we applied Grimme's dispersion with Becke–Johnson damping (GD3BJ) correction.[44] Additionally, the solvent environment was considered using the integrated effective fragment polarizable continuum model (IEFPCM) with a dielectric constant (ε) set at 4.[45] Following geometry optimization, vibrational frequency analyses were

conducted to characterize the stationary points on the potential energy surface and to calculate zero-point energy (ZPE) corrections. Subsequently, the resulting electronic structure underwent topological analysis of the Fukui function (TAFF).[22] The Fukui function is a fundamental concept within DFT, providing insights into global and local molecular reactivity parameters.[46] Sites with higher Fukui function values are favoured as reaction sites. Based on Koopmans' theorem, we determined ionization potential (I), electroaffinity (A), chemical potential (μ), global hardness (η), global softness (S), electronegativity (χ), electrophilicity index (ω), electron acceptor index (ω+), electron donor index (ω–), and net electrophilicity (Δω±).[22] These parameters were derived from the highest occupied molecular orbital (HOMO) and the lowest unoccupied molecular orbital (LUMO), applying topological analysis of the Fukui function.[22]

Acknowledgements

G.P.R. and H.A.B. acknowledge funding from National Scientific and Technical Research Council – Argentina (CONICET) under Projects PIP0111 and PIP090CO, respectively. M.E.R.T., V.P., M.A.F.B., B.L., G.E.F., G.P.R., and H.A.B. are researcher from CONICET. This work partially used computational resources from CCAD-UNC, which is part of SNCAD-MinCyT, Argentina.

Author Contribution Statement

M.E.R.T., M.A.F.B., F.A.G., J.R.A.D., and B.L. conducted the experiments and analyzed the data, reviewed and edited the manuscript. V.P. and G.P.R prepared compounds, analyzed the data, reviewed and edited the manuscript. G.E.F., G.P.R. and H.A.B. supervision, analyzed the data, reviewed and edited the manuscript, project administration and funding acquisition.

Keywords: ADMET, antibacterial, antifungal, sulfonamide, tetrahydroisoquinolines

References

[1] S. McGuire, *Adv. Nutr.* **2015**, *6*, 623-624.

[2] A. Moretti, A. F. Logrieco, A. Susca, *Methods Mol. Biol.* **2017,** *1542*, 3-12.

[3] A. E. Pohland, *Food Addit. Contam.* **1993**, *10*, 17-28.

[4] V. S. Brauer, C.P. Rezende, A. M. Pessoni, R.G. De Paula, K.S. Rangappa, S. C. Nayaka, V. K. Gupta, F. Almeida, *Biomolecules* **2019**, *9*, Article 521.

[5] I. P. Singh, P. Shah, *Expert Opin. Ther.* **2017**, *27*, 17-36.

[6] C. Zhao, K. P. Rakesh, L. Ravidar, W. Y. Fang, H.L. Qin, *Eur. J. Med. Chem.* **2019**, *162*, 679-734.

[7] W. M. Whaley, T.R. Govindachari, 'Organic Reactions', John Wiley & Sons, New York, NY, USA, **1951**, Vol. VI, p. 74-144.

[8] R. Pingaew, S. Prachayasittikul, S. Ruchirawat, V. Prachayasittikul, *Chin. Chem. Lett.* **2013**, *24*, 941-944.

[9] E. X. Aguilera Palacios, V. Palermo, A. G. Sathicq, L.R. Pizzio, G. P. Romnelli, *Catalysts* **2022,** *12*, Article 1155.

[10] F. F. Bamoharram, M. M. Heravi, M. Roshani, M. Jahangir, A. Gharib, *Appl. Catal., A* **2006**, *302*, 42-47.

[11] M. M. Heravi, Z. Faghihi, *J. Iran. Chem. Soc.* **2014**, *11*, 209-224.

[12] G. P. Romanelli, D.M. Ruiz, J. C. Autino, H. E. Giaccio, *Mol. Divers.* **2010**, *14*, 803-807.

[13] D. Banfi, L. Patiny, *Chimia* **2008**, *62*, 280-281.

[14] C. M. Breneman, L.W. Weber, *Can. J. Chem.* **1996**, *74*, 1271-1282.

[15] A. Vigorito, C. Calabrese, A. Maris, D. Loru, I. Pena, M. E. Sanz, S. Melandri, *Molecules* **2022**, Article 2820.

[16] J. S. Delaney, *J. Chem. Inf. Comput. Sci.* **2004**, *44*, 1000-1005.

[17] A. Daina, O. Michielin, V. Zoete, *Sci. Rep.* **2017**, *7*, Article 42717.

[18] L. Di, *Expert Opin. Drug Metab. Toxicol.* **2014**, *10*, 379-393.

[19] M. N. Drwal, P. Banerjee, M. Dunkel, M. R. Wettig, R. Preissner, *Nucleic Acids Res.* **2014**, *42*, W53-58.

[20] S. Singh, N. Singh, V. Kumar, S. Datta, A. B. Wani, D. Singh, K. Singh, J. Singh, *Environ. Chem. Lett.* **2016**, *14*, 317-329.

[21] K. Fukui, Chemical Reactivity Theory, Springer Berlin Heidelberg, Berlin, Heidelberg, **1975**, p. 8-9.

[22] P. Fuentealba, E. Florez, W. Tiznado, *J. Chem. Theory Comput.* **2010**, *6*, 1470-1478.

[23] P. Geerlings, F. De Proft, W. Langenaeker, *Chem. Rev.* **2003**, *103*, 1793-1874.

[24] P. K. Chattaraj, A. Chakraborty, S. Giri, *J. Phys. Chem. A* **2009**, *113*, 10068-10074.

[25] R. M. Lopachin, T. Gavin, A. Decaprio, D. S. Barber, *Chem. Res. Toxicol.* **2012**, *25*, 239-251.

[26] P. K. Chattaraj, *J. Phys. Chem. A* **2001**, *105*, 511-513.

[27] I. Chataigner, C. Panel, H. Gérard, S.R. Piettre, *Chem. Commun.* **2007**, *31*, 3288-3290.

[28] M. E. Beck, *J. Chem. Inf. Model.* **2005**, *45*, 273-282.

[29] M. Newcomb, R. E. Chandrasena, *Biochem. Biophys. Res. Commun.* **2005**, *338*, 394-403.

[30] O. O. Orazi, R. A. Corral, H. Giaccio, *J. Chem. Soc., Perkin Trans. 1* **1986**, *1*, 1977-1982.

[31] J. L. Jios, G.P. Romanelli, J. C. Autino, H.E. Giaccio, H. Duddeck, M. Wiebcke, *Magn. Reson. Chem.* **2005**, *43*, 1057-1062.

[32] M. Natsume, S. Kumadaki, K. Kiuchi, *Chem. Pharm. Bull.* **1972**, *20*, 1592-1595.

[33] D. M. Ruiz, G. P. Romanelli, P. G. Vázquez, J. C. Autino, *Appl. Catal., A* **2010**, *374*, 110-119.

[34] R. Humphries, A. M. Bobenchik, J. A. Hindler, A. N. Schuetz, *J. Clin. Microbiol.* **2021**, *59*, e0021321.

[35] C. A. Lipinski, F. Lombardo, B. W. Dominy, P. J. Feeney, *Adv. Drug Deliv. Rev.* **1997**, *23*, 3-25.

[36] C. A. Lipinski, *Drug Discov. Today Technol.* **2004**, 1, 337-341.

[37] G. Xiong, Z. Wu, J. Yi, L. Fu, Z. Yang, C. Hsieh, M. Yin, X. Zeng, C. Wu, A. Lu, X. Chen, T. Hou, D. Cao, *Nucleic Acids Res.* **2021**, *49*, W5-W14.

[38] D. E. V. Pires, T. L. Blundell, D. B. Ascher, *J. Med. Chem.* **2015**, *58*, 4066-4072.

[39] P. Banerjee, A. O. Eckert, A. K. Schrey, R. Preissner, *Nucleic Acids Res.* **2018**, *46*, W257-W263.

[40] P. Banerjee, F. O. Dehnbostel, R. Preissner, *Front. Chem.* **2018**, *6*, Article 362.

[41] M. J. Frisch, G. W. Trucks, H. B. Schlegel, G. E. Scuseria, M. A. Robb, J. R. Cheeseman, G. Scalmani, V. Barone, G. A. Petersson, H. Nakatsuji, X. Li, M. Caricato, A. V. Marenich, J. Bloino, B. G. Janesko, R. Gomperts, B. Mennucci, H. P. Hratchian, J. V. Ortiz, A. F. Izmaylov, J. L. Sonnenberg, Williams, F. Ding, F. Lipparini, F. Egidi, J. Goings, B. Peng, A. Petrone, T. Henderson, D. Ranasinghe, V. G. Zakrzewski, J. Gao, N. Rega, G. Zheng, W. Liang, M. Hada,

M. Ehara, K. Toyota, R. Fukuda, J. Hasegawa, M. Ishida, T. Nakajima, Y. Honda, O. Kitao, H. Nakai, T. Vreven, K. Throssell, J.A. Montgomery Jr., J. E. Peralta, F. Ogliaro, M. J. Bearpark, J. J. Heyd, E. N. Brothers, K. N. Kudin, V. N. Staroverov, T. A. Keith, R. Kobayashi, J. Normand, K. Raghavachari, A. P. Rendell, J. C. Burant, S. S. Iyengar, J. Tomasi, M. Cossi, J. M. Millam, M. Klene, C. Adamo, R. Cammi, J. W. Ochterski, R. L. Martin, K. Morokuma, O. Farkas, J. B. Foresman, D. J. Fox, Gaussian 16 Rev. C.01, Programm for electronic structure modeling, Gaussian, Inc., Wallingford CT, **2016**.

[42] A. D. Becke, *J. Chem. Phys.* **1993**, *98*, 5648-5652.

[43] W. J. Hehre, R. Ditchfield, J. A. Pople, *J. Chem. Phys.* **1972**, *56*, 2257-2261.

[44] H. Schroder, A. Creon, T. Schwabe, *J. Chem. Theory Comput.* **2015**, *11*, 3163-3170.

[45] P. Bandyopadhyay, M. S. Gordon, B. Mennucci, J. Tomasi, *J. Chem. Phys.* **2002**, *116*, 5023-5032.

[46] R. G. Parr, W. Yang, *J. Am. Chem. Soc.* **1984**, *106*, 4049-4050.

Graphical Abstract

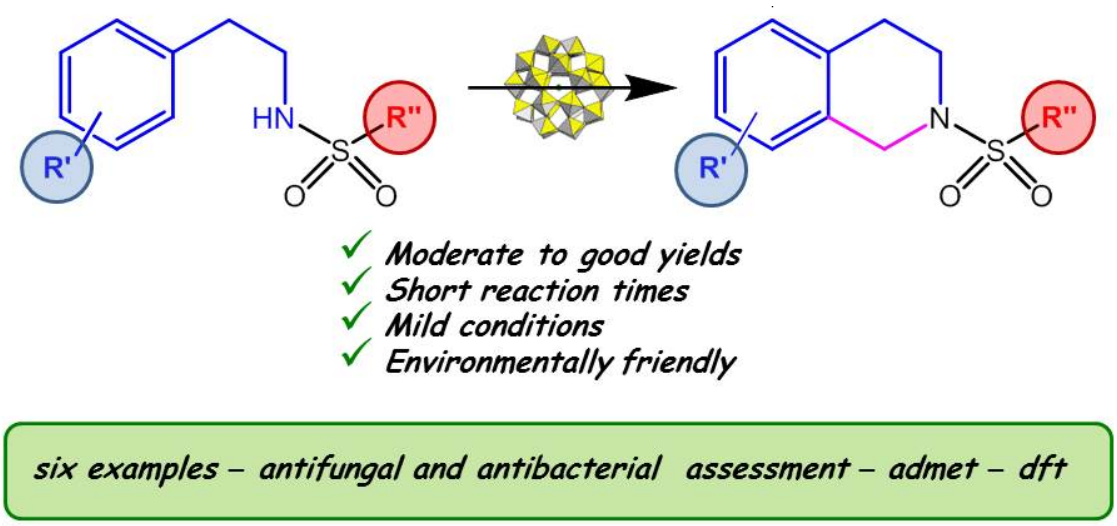

Twitter Text

@noticiasUNSL

@fqbf_unsl

@ConicetSanLuis

@CINDECA

@exatcas_unlp

@CONICETLaPlata